Analysis of Fault Location Algorithms for Parallel Transmission Lines with Series Compensation

M.M. Saha, K. Wikström
ABB Automation Products AB
Västerås, Sweden

E. Rosolowski, J. Izykowski
Wroclaw University of Technology
Wroclaw, Poland

R. Dutra
Furnas Centrais Electricas S.A.
Rio de Janeiro, Brasil

Abstract - **One-end fault location techniques for series-compensated parallel lines are investigated. First, the basic fault location algorithm is presented briefly. Then, the new concept overcoming the drawbacks of the basic algorithm is delivered. The ATP-EMTP program for equivalencing of Series Capacitors (SCs) equipped with Metal Oxide Varistors (MOVs) is presented. Reliable fault data for evaluation of accuracy of the analyzed algorithms has been generated with the developed detailed ATP-EMTP model of series-compensated parallel lines including the measurement channels. The presented results illustrate effectiveness and high accuracy of the new fault location algorithm being distinctive in no requiring the impedance data of the equivalent supplying systems and avoiding of pre-fault measurements.**

Keywords: Parallel Transmission Lines, Capacitor Compensation, ATP-EMTP, Models, Fault Location.

I. INTRODUCTION

Parallel series-compensated lines appear as very important links between energy generation and consumption regions. Such lines exhibit the advantages relevant for both the parallel arrangement and for the series capacitor compensation itself [1, 2]. However, they are considered as extremely difficult for protective relaying as well as for locating faults for inspection and repair purposes [1-3]. Series Capacitors (SCs) installed in the lines are equipped - for overvoltage protection - with nonlinear Metal-Oxide Varistors (MOVs). In consequence, the measurement differs substantially in comparison to the traditional lines case - in both, the static and dynamic characters.

Accurate fault location for parallel power transmission lines with series compensation requires compensating for remote infeed effect under resistive faults, mutual coupling between lines as well as for series compensation effect itself. The basic fault location algorithm dedicated for parallel series-compensated lines coping with all these the effects has been developed and presented in [3]. This was a direct extension of the algorithm developed earlier for a single series-compensated line. Both the location methods are categorized as the one-end techniques. Their main drawback relies in requirement of the impedance data for the equivalent systems behind the line terminals and for the possible extra link between the substations. However, impedances of the equivalent systems can undergo fluctuations during evolving faults and impedance for the remote system can not be measured locally. Possible mismatch between the representative value of the remote system impedance provided for the location algorithm and its actual value causes additional errors in fault location. Moreover, the basic algorithm requires pre-fault measurements, which in some cases can be unreliable or even unavailable. Thus, avoiding of using pre-fault quantities is also highly desirable.

First, the basic location algorithm is presented. Then, the new concept for fault location in series-compensated parallel lines is stated. The delivered new fault location algorithm is derived with considering the healthy line path as the connective medium between the local and the remote terminals of parallel lines during fault occurrence. As a result of that the aforementioned drawbacks of the basic method are overcome.

The presented algorithms are derived for series-compensated parallel lines but after adequate setting they can be adapted to uncompensated parallel lines as well.

II. BASICS OF THE FAULT LOCATION TECHNIQUES

Series-compensated parallel lines as shown in Figures 1, 2 are taken for the analysis. Both the lines in this arrangement are compensated with *3*-phase banks of SCs equipped with MOVs installed at distance *p* [pu] from the station *A*.

Distinctive features of the presented fault location algorithms summarize as follows:

- phase coordinates approach [3, 4] for describing parallel lines, representing SCs&MOVs and a fault is utilized,
- two characteristic fault spots (Figures 1, 2) are considered and thus two subroutines are used in the algorithms: *Subroutine 1* (Fig. 1) for locating faults behind the SCs&MOVs with additional discrimination of the faults overreaching the line length (denoted in Fig. 1 as F1a); the sought fault distance (x_1 [pu]) satisfies: $x_1 > p$, *Subroutine 2* (Fig. 2) for locating faults in front of the SCs&MOVs; the sought fault distance (x_2 [pu]) satisfies: $x_2 < p$.
- separate selection procedure is applied to obtain the correct estimate out of the two conditional solutions delivered by the subroutines 1, 2,
- shunt capacitances of parallel lines are neglected, however, to improve fault location accuracy in case of long lines the capacitances may be accounted for,
- the recorded voltage and current data cover the time window before firing the air-gaps, which are in parallel with MOVs (note that air-gaps are not shown in Figures 1, 2),
- fault detection and classification is provided by a protective relay or by separate procedures of the locator.

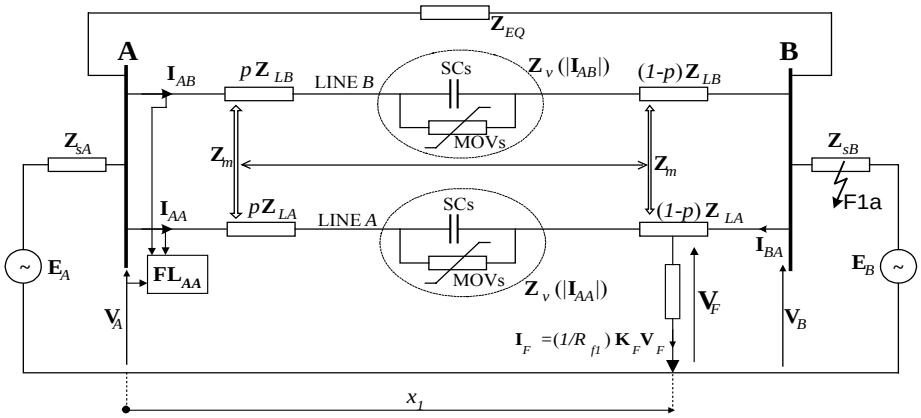

Fig. 1. Model of parallel lines for faults occurring behind SCs&MOVs (Subroutine 1)

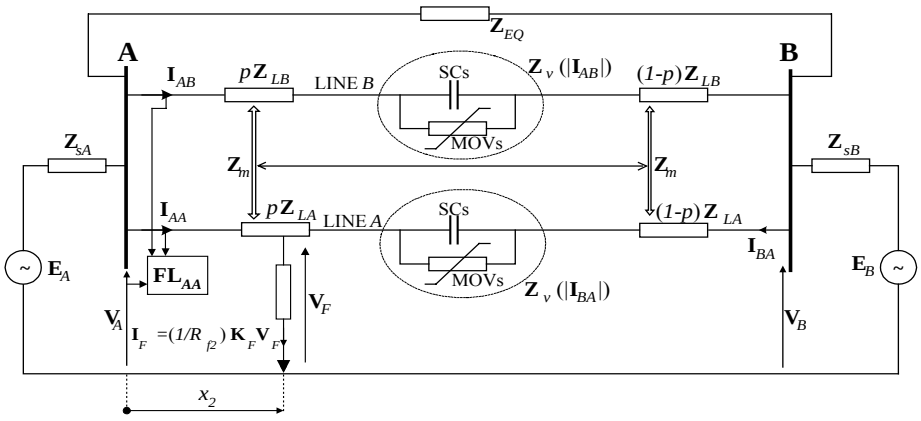

Fig. 2. Model of parallel lines for faults occurring in front of SCs&MOVs (Subroutine 2)

Parallel lines model and the way of representing SCs&MOVs and a fault in the algorithms follow. All the symbols, except distance to fault (x_1 or x_2) and fault resistance (R_{f1} or R_{f2}), stand for complex numbers, either impedances or phasors, while the matrix quantities are bold-type written.

A. Parallel lines model

Neglecting shunt capacitances the voltage drop across the segment of the length x [pu] of the line A (Figures 1, 2) is determined with the matrix formula:

$$\Delta\mathbf{V}_{LAx} = x\left(\mathbf{Z}_{LA}\mathbf{I}_{AA} + \mathbf{Z}_m\mathbf{I}_{AB}\right) \qquad (1)$$

in which the self ($\mathbf{Z}_{LA}$) and mutual coupling ($\mathbf{Z}_m$) matrix impedances could be - in general - of asymmetric form. However, for completely transposed parallel lines holds:

$$\mathbf{Z}_{LA} = \begin{bmatrix} Z_{LAs} & Z_{LAm} & Z_{LAm} \\ Z_{LAm} & Z_{LAs} & Z_{LAm} \\ Z_{LAm} & Z_{LAm} & Z_{LAs} \end{bmatrix}, \mathbf{Z}_m = \frac{1}{3}\begin{bmatrix} Z_{0m} & Z_{0m} & Z_{0m} \\ Z_{0m} & Z_{0m} & Z_{0m} \\ Z_{0m} & Z_{0m} & Z_{0m} \end{bmatrix} \qquad (2)$$

Self (s) and mutual (m) components of $\mathbf{Z}_{LA}$ (2) are determined by the zero (*0*) and positive (*1*) sequence data:

$$Z_{LAs} = \frac{1}{3}\left(Z_{LA0} + 2Z_{LA1}\right), \quad Z_{LAm} = \frac{1}{3}\left(Z_{LA0} - Z_{LA1}\right),$$

Z_{0m} - mutual coupling zero sequence impedance.

B. Representation of SCs and MOVs

Typical voltage-current characteristic of an MOV, waveforms for a voltage drop across SC&MOV, currents flowing through SC and MOV branches are shown in Fig.3.

A bank of parallel branches of a SC and its MOV is represented for the fundamental frequency phasors by equivalent resistance and reactance, connected in series (Fig.4a). The program containing the ELECTRICAL NETWORK and the MODELS units of the ATP-EMTP package [5] (Fig. 4b) has been developed for determining the equivalents. The equivalent resistance and reactance are obtained as dependent on amplitude of current entering the original circuit. This is achieved by scanning over the wide range for amplitude of the fault current entering the SC&MOV.

Equivalent resistance and reactance, determined for different compensation rates (*60, 70, 80* %) of the analyzed *400*kV, *300*km parallel lines are presented in Figures 4c, d.

The SCs&MOVs are represented in the algorithm by the impedance matrix dependent on amplitudes of currents:

$$\mathbf{Z}_{\mathbf{V}}\left(|\mathbf{I}_{\mathbf{V}}|\right) = \begin{vmatrix} Z_V\left(|I_{Va}|\right) & 0 & 0 \\ 0 & Z_V\left(|I_{Vb}|\right) & 0 \\ 0 & 0 & Z_V\left(|I_{Vc}|\right) \end{vmatrix} \qquad (3)$$

where I_{va}, I_{vb}, I_{vc} are phasors of the currents flowing through the banks of SC&MOV in particular phases and by "$|\ |$" the amplitude of the phasor is denoted.

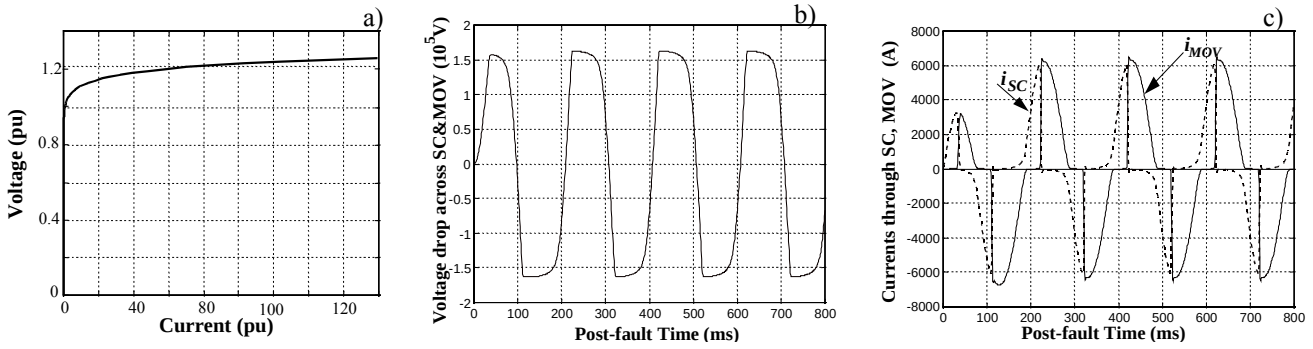

Fig. 3. MOV operation: a) MOV characteristic, b) voltage drop across SC&MOV, c) currents flowing through SC, MOV.

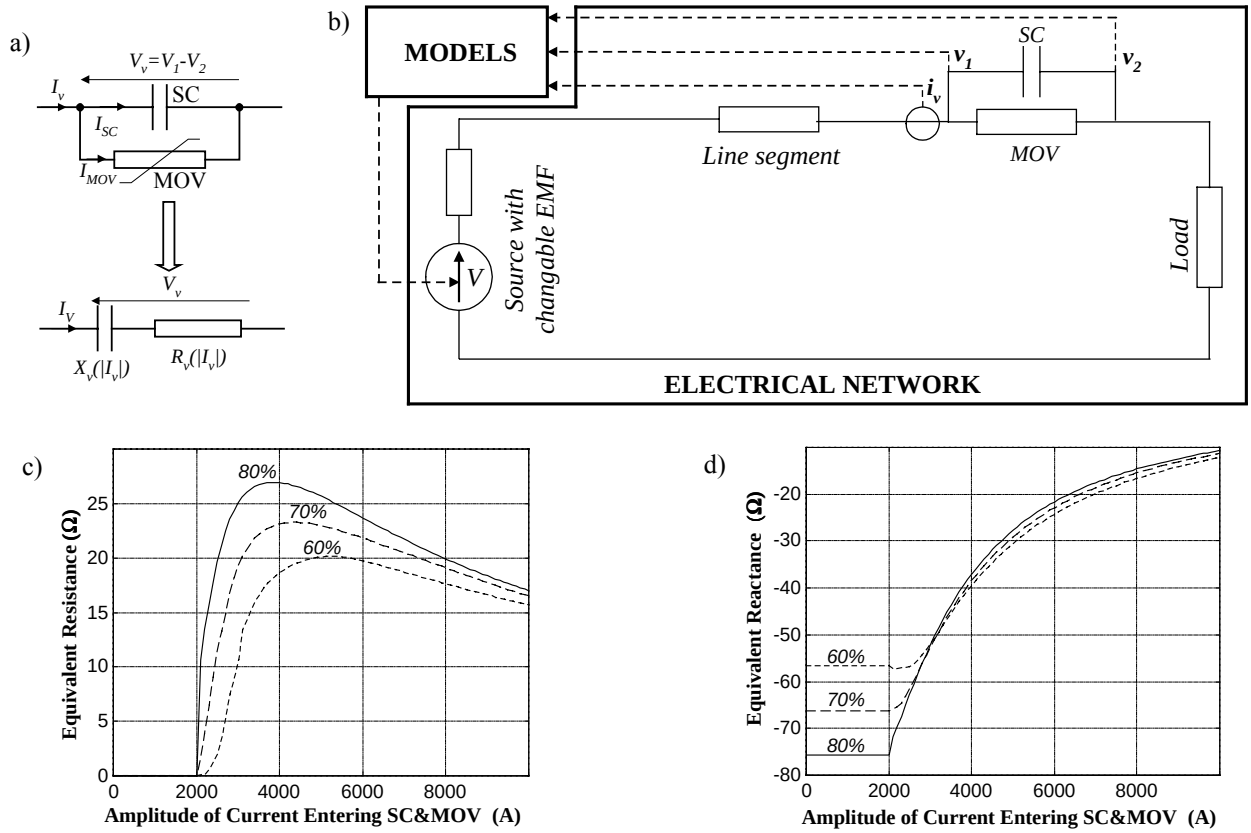

Fig. 4. Fundamental frequency equivalencing of SC&MOV circuit: a) principle of equivalencing, b) use of ATP-EMTP for equivalencing, c) equivalent resistance, d) equivalent reactance.

C. Fault model

In order to take into account a voltage drop across a fault path the total fault current has to be determined. Both, local currents ($\mathbf{I}_{AA}$) and remote currents ($\mathbf{I}_{BA}$) from the faulted line contribute to the total fault current (under neglecting shunt capacitances of a line):

$$\mathbf{I}_F = \mathbf{I}_{AA} + \mathbf{I}_{BA} \tag{4}$$

A general fault model is utilized in the presented fault location algorithms. This model is stated in matrix notation as follows:

$$\mathbf{I}_F = \frac{1}{R_f}\mathbf{K}_F\mathbf{V}_F \tag{5}$$

$\mathbf{V}_F$, $\mathbf{I}_F$ - vectors of voltages and currents at fault,

R_f - aggregated value of fault resistance,

$\mathbf{K}_F$ - fault matrix built upon the fault type.

Matrix $\mathbf{K}_F$ is obtained with the following two steps procedure:

1. compute:

$$k_{ij} = \begin{cases} -1 & \text{if } i \text{ and } j \text{ involved in fault} \\ 0 & \text{otherwise} \end{cases} \qquad i, j = a, b, c \tag{5a}$$

2. adjust the diagonal elements using the formula:

$$k_{ii} = \sum_{j=a}^{j=c} \left| k_{ij} \right| \quad i = a, b, c \tag{5b}$$

III. BASIC FAULT LOCATION ALGORITHM

A. Subroutine 1 – for faults behind SCs&MOVs

In this case a faults is considered as behind SCs&MOVs but not overreaching the line length (Fig. 1). The difference of EMFs at both sides is to be determined from the post-fault as well as from pre-fault conditions (the subscript *pre* stands for all the pre-fault quantities):

$$\begin{aligned}\mathbf{E}_A-\mathbf{E}_B=&\left(\mathbf{Z}_{sA}+x_1\mathbf{Z}_{LA}+\mathbf{Z}_v\left(\left|\mathbf{I}_{AA}\right|\right)\right)\mathbf{I}_{AA}+\\&-\left((1-x_1)\mathbf{Z}_{LA}+\mathbf{Z}_{sB}\right)\mathbf{I}_{BA}+\left(\mathbf{Z}_{sA}+\mathbf{Z}_{sB}+\mathbf{Z}_m\right)\mathbf{I}_{AB}\end{aligned}\tag{6}$$

$$\begin{aligned}\mathbf{E}_A-\mathbf{E}_B=&\left(\mathbf{Z}_{sA}+\mathbf{Z}_{sB}+\mathbf{Z}_{LA}+\mathbf{Z}_v\left(\left|\mathbf{I}_{AA\_pre}\right|\right)\right)\mathbf{I}_{AA\_pre}+\\&+\left(\mathbf{Z}_{sA}+\mathbf{Z}_{sB}+\mathbf{Z}_m\right)\mathbf{I}_{AB\_pre}\end{aligned}\tag{7}$$

Voltage drop across a fault path is determined as:

$$\mathbf{V}_F=\mathbf{V}_A-x_1\mathbf{Z}_{LA}\mathbf{I}_{AA}-\mathbf{Z}_v(|\mathbf{I}_{AA}|)\mathbf{I}_{AA}-x_1\mathbf{Z}_m\mathbf{I}_{AB}\tag{8}$$

The set of matrix equations ((6) - (8)) together with the fault model ((4) - (5)) yield the matrix equation for the fault distance (x_1) and aggregated fault resistance (R_{f1}):

$$\mathbf{A}_c x_1^{\,2}-\mathbf{B}_c x_1+\mathbf{C}_c-\mathbf{D}_c R_{f1}=0\tag{9}$$

where $\mathbf{A}_c$, $\mathbf{B}_c$, $\mathbf{C}_c$, $\mathbf{D}_c$ are the vectors depending on the impedance parameters of a line and equivalent systems at the line terminals as well as the local measurements.

The matrix formula (9) can be transformed to the scalar form and solved for a sought fault distance. This is shown in the next section for the improved location algorithm.

Faults occurring in the remote system (fault F1a in Fig.1) which are also behind the SCs&MOVs can be discriminated by considering the following vector:

$$\begin{aligned}\mathbf{D}=&\left(\mathbf{Z}_{LA}+\mathbf{Z}_v\left(|\mathbf{I}_{AA}|\right)-\mathbf{Z}_m\right)\mathbf{I}_{AA}+\\&-\left(\mathbf{Z}_{LB}+\mathbf{Z}_v\left(|\mathbf{I}_{AB}|\right)-\mathbf{Z}_m\right)\mathbf{I}_{AB}\end{aligned}\tag{10}$$

which for such faults has all the components equal to zeroes (in practice certain threshold is to be applied for that).

B. Subroutine 2 - faults in front of SCs&MOVs

The case of a fault between the substation and the SCs&MOVs (Fig. 2) is more involved because the current flowing through the SCs&MOVs is not directly available to the one-end locator and thus ought to be estimated.

In this case the following applies to the faulty network:

$$\begin{aligned}\mathbf{E}_A-\mathbf{E}_B=&\left(\mathbf{Z}_{sA}+x_2\mathbf{Z}_{LA}\right)\mathbf{I}_{AA}+\left(\mathbf{Z}_{sA}+\mathbf{Z}_{sB}+\mathbf{Z}_m\right)\mathbf{I}_{AB}+\\&-\left((1-x_2)\mathbf{Z}_{LA}+\mathbf{Z}_{sB}+\mathbf{Z}_v\left(\left|\mathbf{I}_{BA}\right|\right)\right)\mathbf{I}_{BA}\end{aligned}\tag{11}$$

$$\mathbf{V}_F=\mathbf{V}_A-x_2\mathbf{Z}_{LA}\mathbf{I}_{AA}-x_2\mathbf{Z}_m\mathbf{I}_{AB}\tag{12}$$

The model of the pre-fault network (7) and the fault model ((4) - (5)) remain valid. In consequence, one also obtains the quadratic equation as (9), but an iterative numerical solution is required because its coefficients depend on the unknown current from the remote substation B.

IV. IMPROVED FAULT LOCATION ALGORITHM

This algorithm also considers two characteristic fault spots and thus again consists of two subroutines for a fault as seen behind or in front of SCs&MOVs, respectively.

A. Subroutine 1 – for faults behind SCs&MOVs

Both, the faulted and the healthy line paths are considered for deriving this algorithm:

- for the faulted line:

$$\mathbf{V}_F=\mathbf{V}_A-x_1\mathbf{Z}_{LA}\mathbf{I}_{AA}-\mathbf{Z}_v(|\mathbf{I}_{AA}|)\mathbf{I}_{AA}-x_1\mathbf{Z}_m\mathbf{I}_{AB}\tag{13}$$

$$\mathbf{V}_F=\mathbf{V}_B-(1-x_1)\mathbf{Z}_{LA}\mathbf{I}_{BA}+(1-x_1)\mathbf{Z}_m\mathbf{I}_{AB}\tag{14}$$

- for the healthy line:

$$\begin{aligned}\mathbf{V}_A-\mathbf{V}_B=&\left(\mathbf{Z}_{LB}+\mathbf{Z}_v(|\mathbf{I}_{AB}|)\right)\mathbf{I}_{AB}+\\&+x_1\mathbf{Z}_m\mathbf{I}_{AA}-(1-x_1)\mathbf{Z}_m\mathbf{I}_{BA}\end{aligned}\tag{15}$$

The formulae (13) - (15) together with (4) – (5) yield the matrix equation:

$$\mathbf{A}_c x_1^{\,2}-\mathbf{B}_c x_1+\mathbf{C}_c-\mathbf{D}_c R_{f1}=0\tag{16}$$

in which the vectors (*3x1*) are determined as follows:

$$\begin{aligned}\mathbf{A}_c&=\left(\mathbf{Z}_m-\mathbf{Z}_{LA}\right)\mathbf{K}_F\left(\mathbf{Z}_{LA}\mathbf{I}_{AA}+\mathbf{Z}_m\mathbf{I}_{AB}\right)\\\mathbf{C}_c&=\left(\mathbf{Z}_m-\mathbf{Z}_{LA}\right)\mathbf{K}_F\left(\mathbf{V}_A-\mathbf{Z}_v(|\mathbf{I}_{AA}|)\mathbf{I}_{AA}\right)\\\mathbf{B}_c&=\mathbf{A}_c+\mathbf{C}_c\\\mathbf{D}_c&=\left(\mathbf{Z}_m-\mathbf{Z}_{LA}-\mathbf{Z}_v(|\mathbf{I}_{AA}|)\right)\mathbf{I}_{AA}-\left(\mathbf{Z}_m-\mathbf{Z}_{LB}-\mathbf{Z}_v(|\mathbf{I}_{AB}|)\right)\mathbf{I}_{AB}\end{aligned}$$

Transforming the matrix formula (16) to the scalar equation can be accomplished by multiplying both sides of (16) by the vector $\mathbf{D}_c^{\,T}/(\mathbf{D}_c^{\,T}\mathbf{D}_c)$ (*T* denotes matrix transposition). As a result the quadratic equation is obtained:

$$Ax_1^{\,2}-Bx_1+C-R_{f1}=0\tag{17}$$

where: *A, B, C* are the complex scalars depending on the impedance data of parallel lines only and the local measurements of voltages and currents from the faulted and from the healthy lines.

Faults occurring in the remote system (fault F1a in Fig. 1) can be discriminated by considering the vector (10).

B. Subroutine 2 – for faults in front of SCs&MOVs

In this case the formulae (4), (5) are still valid but (13) – (15) have to be replaced by the relations:

- for the faulted line:

$$\mathbf{V}_F=\mathbf{V}_A-x_2\mathbf{Z}_{LA}\mathbf{I}_{AA}-x_2\mathbf{Z}_m\mathbf{I}_{AB}\tag{18}$$

$$\mathbf{V}_F=\mathbf{V}_B-(1-x_2)\left(\mathbf{Z}_{LA}\mathbf{I}_{BA}-\mathbf{Z}_m\mathbf{I}_{AB}\right)-\mathbf{Z}_v(|\mathbf{I}_{BA}|)\mathbf{I}_{AA}\tag{19}$$

- for the healthy line:

$$\begin{aligned}\mathbf{V}_A-\mathbf{V}_B=&\left(\mathbf{Z}_{LB}+\mathbf{Z}_v(|\mathbf{I}_{AB}|)\right)\mathbf{I}_{AB}+\\&+x_2\mathbf{Z}_m\mathbf{I}_{AA}-(1-x_2)\mathbf{Z}_m\mathbf{I}_{BA}\end{aligned}\tag{20}$$

The set of formulae (4) - (5), (18) – (20) yields:

$$\mathbf{A}_c x_2^{\,2}-\mathbf{B}_c x_2+\mathbf{C}_c-\mathbf{D}_c R_{f2}=0\tag{21}$$

in which the vectors (*3x1*) are determined as follows:

$$\begin{aligned}\mathbf{A}_c&=\left(\mathbf{Z}_m-\mathbf{Z}_{LA}\right)\mathbf{K}_F\left(\mathbf{Z}_{LA}\mathbf{I}_{AA}+\mathbf{Z}_m\mathbf{I}_{AB}\right)\\\mathbf{B}_c&=\left(\mathbf{Z}_m-\mathbf{Z}_{LA}\right)\mathbf{K}_F\left(\mathbf{V}_A+\mathbf{Z}_{LA}\mathbf{I}_{AA}+\mathbf{Z}_m\mathbf{I}_{AB}\right)\\&\quad-\mathbf{Z}_v(|\mathbf{I}_{BA}|)\mathbf{K}_F\left(\mathbf{Z}_{LA}\mathbf{I}_{AA}+\mathbf{Z}_m\mathbf{I}_{AB}\right)\\\mathbf{C}_c&=\left(\mathbf{Z}_m-\mathbf{Z}_{LA}-\mathbf{Z}_v(|\mathbf{I}_{BA}|)\right)\mathbf{K}_F\mathbf{V}_A\\\mathbf{D}_c&=\left(\mathbf{Z}_m-\mathbf{Z}_{LA}-\mathbf{Z}_v(|\mathbf{I}_{BA}|)\right)\mathbf{I}_{AA}-\left(\mathbf{Z}_m-\mathbf{Z}_{LB}-\mathbf{Z}_v(|\mathbf{I}_{AB}|)\right)\mathbf{I}_{AB}\end{aligned}$$

Matrix formula (16) can be transformed to the scalar quadratic equation, which is of the same form as (17) obtained for the subroutine 1.

C. Selection procedure

Locating a fault with respect to the SCs&MOVs (Fig. 1, 2) narrows to the selection of the correct pair (x,R_f) out of two alternatives (x_1,R_{f1}) and (x_2,R_{f2}). The selection procedure is based on appropriate aggregation of the criteria values, which are estimated with both the subroutines:

- aggregated fault resistance R_f (*applicable for all the fault types*): the smaller positive value of R_f indicates the valid subroutine while the negative value rejects it,
- amplitudes of currents from healthy phases of the fault path (*applicable for all the fault types except three-phase symmetrical faults*): the subroutine which gives lower amplitudes (ideally zeroes) is taken as the valid one.

IV. TESTING AND EVALUATING THE ALGORITHM

The detailed ATP-EMTP model of *400* kV, *300* km series-compensated parallel lines network has been developed for generating reliable fault data to be used in testing and evaluating the algorithms. It was assumed that SCs are installed at *p=0.5* pu and compensation rate is *70* %.

The supplying systems at both the substations were taken as identical with the impedance data:

$\underline{Z}_{1sA} = 15\,\Omega\angle 85$ deg , $\underline{Z}_{0sA} = 26.7\,\Omega\angle 85$ deg

and the EMFs at the side B were delayed by *30*deg with respect to the side A.

The MOVs with the common approximation of the *v-i* characteristic (Fig. 3a) were taken:

$$\frac{i}{P} = \left(\frac{v}{V_{REF}}\right)^q \qquad (22)$$

with the parameters: *q=23*, *P=1* kA, V_{REF} *=150* kV.

The model included the Capacitive Voltage Transformers (CVTs) and the Current Transformers (CTs). The analog filters were also implemented using the *2*nd order Butterworth approximation.

The phasors were estimated with the use of the DFT algorithm working with *20* samples per cycle.

Example of fault location in series-compensated parallel lines (Figures 5, 6, 7) has been performed for the fault:

- fault type: phase-to-ground (a-g),
- fault resistance: *10* Ω,
- fault location: at *0.833* pu, thus behind the SCs&MOVs as seen by the considered fault locator FL_{AA} from the substation A (Fig. 1).

Nature of the transients in the fault locator input signals (Fig. 5a, b, c) is typical for the fault case when the SC&MOV are included in a fault loop. Fault location (Fig. 6a, b, c) has been performed in the following ways:

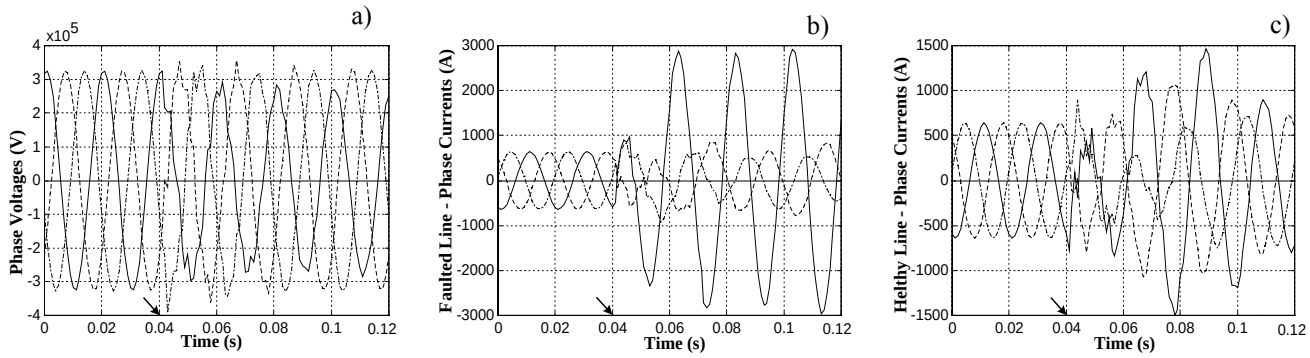

Fig. 5. The example of fault location in parallel lines - waveforms of input signals of fault locator: a) phase voltages, b) phase currents from the faulted line, c) phase currents from the healthy line.

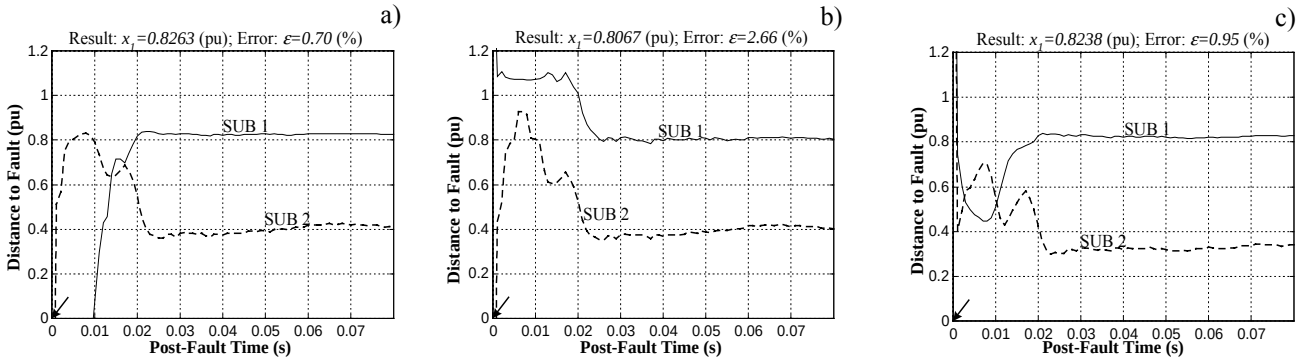

Fig. 6. The example of fault location in parallel lines - location performed with:
a) the basic algorithm under no mismatch for the remote source impedance,
b) the basic algorithm under *50* % mismatch for the remote source impedance,
c) the improved algorithm.

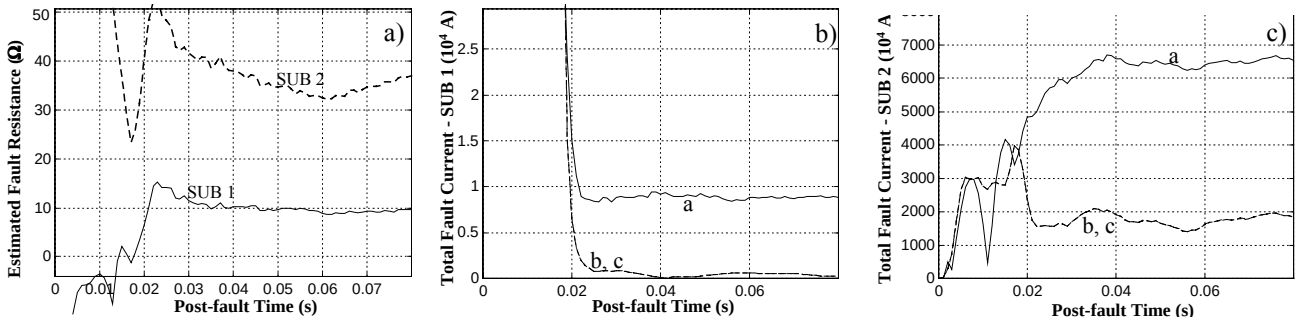

Fig. 7. The example of fault location in parallel lines – selection of the valid subroutine on the base of the estimated criteria values for: a) fault resistance, b) amplitudes of fault path currents (with the subroutine 1), c) amplitudes of fault path currents (with the subroutine 2).

- Fig. 6a – using the basic algorithm with providing exact impedances for the equivalent systems: the estimated fault distance (*0.8263* pu) exhibits the error of *0.70* %,
- Fig. 6b – using the basic algorithm with providing exact impedance for the local equivalent system and *50* % higher for the remote system: the estimated distance (*0.8067* pu) exhibits the error of 2.66%,
- Fig. 6c – using the improved algorithm: the estimated fault distance (*0.8238* pu) exhibits the error of *0.95* %

The basic location algorithm is sufficiently accurate for vast majority of simulated faults, especially when impedances for the equivalent systems are accurately known (Fig. 6a). The mismatch with respect to remote system impedance can cause the extra errors, as for example for the case from Fig. 6b it reaches around *2* %. The delivered improved location algorithm (the case of Fig. 6c) is superior with respect to this, as high accuracy is achieved even if a compensation for shunt capacitances of a line was not accomplished in this case. Further improvement of accuracy can be achieved by incorporating the compensation.

Distance to a fault in the considered examples from Fig. 6a, b, c is estimated with the subroutine 1 (SUB 1) which is selected here as the valid. Fig. 7 presents how this selection is performed. Both estimated criteria quantities, the fault resistance and the amplitudes of fault path currents from the healthy phases (for the considered a-g fault the phases b, c are the healthy phases) support selection of the subroutine 1 as the valid.

V. CONCLUSIONS

The basic fault location algorithm for series-compensated parallel lines has been presented. With the aim of overcoming the drawbacks of this algorithm the new concept for fault location has been formulated. Both the presented algorithms are categorized as one-end methods. The algorithms use two subroutines, which are designated for locating faults behind and in front of SCs&MOVs, respectively. The final estimate is obtained with the separate selection procedure.

The new fault location algorithm has been derived with considering the healthy line path in addition to the faulted line circuit. In consequence of that, the algorithm does not require impedances of the equivalent systems behind both terminals of parallel lines and for the possible extra link between the substations. Moreover, usage of pre-fault quantities is avoided in the algorithm.

ATP-EMTP program containing the ELECTRICAL NETWORK and the MODELS units developed for equivalencing of SC&MOV circuit has been presented.

The delivered algorithms have been extensively evaluated with the fault data generated with ATP-EMTP versatile simulations. The analysis has shown improvement of accuracy of fault location with use of the new algorithm - in comparison to the basic method. This is illustrated with the attached examples of fault location where the improvement of accuracy reaches 2%.

The examples of fault location considered in this paper deal with perfectly transposed parallel lines. However, the applied phase coordinates approach to the network description enables to locate faults in untransposed lines [6] as well.

VI. REFERENCES

[1] CIGRE SC-34 WG-04, *Application guide on protection of complex transmission network configurations*, CIGRE, August 1990.

[2] M.S. Sachdev (coordinator), *Advancements in microprocessor based protection and communication,* IEEE Tutorial, IEEE Publication No. 97TP120-0, 1997.

[3] M.M. Saha, K. Wikstrom, J. Izykowski and E. Rosolowski, "Fault location in uncompensated and series-compensated parallel lines", *Proceedings of PES Winter Meeting*, IEEE Catalog: 00CH37077C, CD-ROM: 0-7803-5938-0, 23-27.01.2000, Singapore.

[4] P.J. Moore, R. Whittard and A.T. Johns, "A novel earth fault location technique utilizing single ended measurements", Proc. of the Stockholm Power Tech Conference, Stockholm, Sweden, June 18-22, 1995, paper SPT IC 12-03-0515, pp. 406-410.

[5] H. Dommel, *ElectroMagnetic Transient Program*, BPA, Portland, Oregon, 1986.

[6] E. Rosolowski, J. Izykowski, M.M. Saha, K. Wikstrom, Effects of transmission line modeling on fault location. Proceedings of EMTP/ATP European Users Group Meeting – EEUG'2000. Wroclaw, Poland, 25-26 September 2000, pp. 109-116.